

Spectral properties and isotope effect in strongly interacting systems: Mott-Hubbard insulator versus polaronic semiconductor

S. Fratini

*Laboratoire d'Etudes des Propriétés Electroniques des Solides, CNRS-BP166-25, Avenue des Martyrs,
F-38042 Grenoble Cedex 9, France*

S. Ciuchi

*Istituto Nazionale di Fisica della Materia and Dipartimento di Fisica Università dell'Aquila, via Vetoio,
I-67010 Coppito-L'Aquila, Italy*

(Received 17 May 2005; revised manuscript received 5 August 2005; published 2 December 2005)

We study the electronic spectral properties in two examples of strongly interacting systems: A Mott-Hubbard insulator with additional electron-boson interactions, and a polaronic semiconductor. An approximate unified framework is developed for the high energy part of the spectrum, in which the electrons move in a random field determined by the interplay between magnetic and bosonic fluctuations. When the boson under consideration is a lattice vibration, the resulting isotope effect on the spectral properties is similar in both cases, being strongly temperature and energy dependent, in qualitative agreement with recent photoemission experiments in the cuprates.

DOI: [10.1103/PhysRevB.72.235107](https://doi.org/10.1103/PhysRevB.72.235107)

PACS number(s): 71.38.-k, 79.60.-i, 74.72.-h

I. INTRODUCTION

A general feature of strongly interacting electron systems is a sizeable suppression of the metallic character, accompanied by a redistribution of the spectral weight from the region close to the Fermi level towards higher energies. In the presence of a strong electron-electron repulsion, for example, incoherent excitations arise far from the Fermi energy in the so-called upper and lower Hubbard bands, at an energy scale which is ruled by the strength U of the interaction. A similar behavior is also found in systems with strong electron-lattice coupling, where the spectral weight is transferred to broad peaks located at $\pm E_p$, the polaron binding energy.

Recent photoemission experiments in the high-Tc cuprates,¹⁻⁴ which are generally described in terms of purely electronic models due to the proximity to a Mott insulating phase, have revealed the existence of an important electron-lattice coupling. This has given rise to intense theoretical work focusing on the excitation spectra in the presence of electron-boson interactions, both in models with⁵⁻⁷ and without⁸⁻¹³ electronic correlations. Of particular interest are those works which focus on isotope effects (IE), since they can disentangle the properties which are directly related to the coupling to the lattice degrees of freedom. For example, it has been found that an anomalous isotope effect on the effective mass arises at the polaron crossover, signaling the breakdown of the Migdal-Eliashberg adiabatic approximation.¹⁴ An enhancement of the IE is also expected in the proximity of a Mott metal-insulator transition, i.e., at intermediate values of the electron-electron repulsion.¹⁵ On the other hand, a strong electronic repulsion suppresses the effects of the lattice dynamics on the low energy excitations near the Fermi level. These persist at high energy, where they amount essentially to a broadening of the electronic spectra.⁵

In this work, we provide an approximate theoretical framework based on the coherent potential approximation

(CPA), which qualitatively describes the high-energy excitation spectra resulting from both electron-electron and electron-boson interactions, treating the fluctuations of magnetic and bosonic origin as a local *static* disorder. Although simplified, the present analytical treatment is able to account for the existence of broad incoherent peaks at high energy, which are a common characteristic of strongly interacting electronic systems.

We analyze two extreme cases which can be important for our general understanding of the problem: (i) A paramagnetic Mott-Hubbard insulator at half-filling, in the presence of an additional local interaction of the electrons with dispersionless bosons and (ii) a polaronic semiconductor, where the physics is solely determined by the electron-boson coupling. In the former case, the validity of our approach relies on the separation of electronic and bosonic energy scales, which is achieved due to a strong electron-electron repulsion. In the latter case, the present CPA results are controlled by direct comparison with an exact solution obtained by dynamical mean field theory (DMFT).¹⁶

The consequences of the electron-boson coupling on the dispersion and width of the high energy features in the spectral function are calculated in both situations, in Secs. II and III, respectively. Particular attention is devoted to the effect of a shift of the boson frequency, as can be achieved through an isotopic substitution if the bosonic mode that couples to the electrons is a lattice vibration, or more generally if it is a collective mode with a sizeable lattice component (in which case a nontrivial IE can still arise, provided that the frequency of the boson is modified by the isotopic substitution). In the present approximation, the IE on the high energy part of the spectrum turns out to be qualitatively similar in the Mott-Hubbard insulator and in the polaronic semiconductor, being mainly determined by the strength of the electron-boson coupling (albeit slightly enhanced by the presence of electronic correlations): In both cases it is strongly tempera-

ture and energy dependent, in agreement with the recently measured IE in the high temperature superconductor $\text{Bi}_2\text{Sr}_2\text{CaCu}_2\text{O}_{8+\delta}$.^{17,18} A tentative analysis of the experimental results, performed in Sec. IV, is compatible with the existence of a moderate electron-phonon coupling in the cuprates.

II. ELECTRON-BOSON COUPLING IN A MOTT-HUBBARD INSULATOR

A. Coherent potential approximation

We study the following Holstein-Hubbard Hamiltonian:

$$H = \sum_{k,\sigma} \epsilon_k c_{k,\sigma}^\dagger c_{k,\sigma} + U \sum_i n_{i,\uparrow} n_{i,\downarrow} - g \sum_{i,\sigma} n_{i,\sigma} (a_i + a_i^\dagger) + \omega_0 \sum_i a_i^\dagger a_i,$$

where electrons in a band with dispersion ϵ_k mutually interact through an on-site repulsion U , and are coupled locally to a dispersionless bosonic mode of frequency ω_0 , with a strength g . We shall set the energy units such that $\hbar = k_B = 1$. We calculate the spectral properties of the above model at half filling, in the paramagnetic phase and in the absence of translational symmetry breaking, in the framework of the coherent potential approximation (CPA).^{19,20} This is suitable for the Mott insulating phase at large U , but also gives a fair description of the high energy incoherent excitations in the correlated metal, provided that the upper and the lower Hubbard bands are well separated from the low energy quasi-particle peak.²¹ The latter, however, is not accessible within this theory, and the position of the chemical potential remains undetermined except at half-filling. Additional features that are not included in the present description are the coherent excited states that arise at low temperature (even in the insulating phase), due to the quantum nature of the magnetic excitations, in an energy range $J \sim t^2/U$ around the Hubbard band edges,²²⁻²⁴ and whose dispersion is strongly reminiscent of spin density waves.

Bearing these limitations in mind, the success of the CPA is that, despite its formal simplicity, it correctly accounts for the high-energy scattering by the randomly distributed magnetic moments. The momentum-integrated Green's function has the form:²⁰

$$G(\omega) = \frac{1}{2} \left[\frac{1}{G_0^{-1}(\omega) - \frac{U}{2}} + \frac{1}{G_0^{-1}(\omega) + \frac{U}{2}} \right] \quad (1)$$

where G_0 is an effective propagator which takes hopping processes into account. It can be eliminated by introducing a local self-energy $\Sigma(\omega)$ through the following self-consistency condition:

$$G(\omega) = \sum_k \frac{1}{\omega - \epsilon_k - \Sigma(\omega)} = \frac{1}{G_0^{-1}(\omega) - \Sigma(\omega)} \quad (2)$$

(in the ‘‘atomic’’ limit, $G_0 = 1/\omega$ and the usual single site propagator is recovered²⁰). For each frequency ω , we are left

with a system of two equations for the two complex unknowns $G(\omega)$ and $\Sigma(\omega)$.

In the presence of a local electron-boson interaction, Eq. (1) can be generalized by introducing an additional field y , which accounts for the random distribution of electronic energies due to the fluctuations of the bosons at different sites⁴⁰

$$G(\omega) = \int \frac{dy}{2} P(y) \left[\frac{1}{G_0^{-1}(\omega) - \frac{U}{2} - y} + \frac{1}{G_0^{-1}(\omega) + \frac{U}{2} - y} \right]. \quad (3)$$

In a system where the on-site electron-electron repulsion directly competes with the attraction induced by the bosons, the formation of bipolarons (and the resulting strong anharmonicities in the boson field)^{25,26} is prevented provided that U is much larger than the polaron binding energy $E_P = g^2/\omega_0$.^{15,27} In this case, we can assume that the boson field obeys the following Gaussian distribution,

$$P(y) = \frac{1}{\sqrt{2\pi\sigma^2}} \exp\left[-\frac{y^2}{2\sigma^2}\right] \quad (4)$$

The variance

$$\sigma^2 = E_P \omega_0 \coth\left(\frac{\omega_0}{2T}\right) \quad (5)$$

is determined either by the thermal fluctuations (at high temperature, $T \gg \omega_0$) or by the quantum fluctuations of the bosons (at low temperature, $T \ll \omega_0$).

Let us emphasize that we have neglected boson renormalization effects which, even in the presence of a strong electron-boson interaction, are suppressed by a sufficiently strong repulsion U .^{15,27} Such effects can in principle be included by taking ω_0 in Eq. (5) equal to the measured boson frequency rather than the bare parameter of eq. (1). However, the present scheme is expected to break down in situations where the bosonic and electronic energy scales become comparable (i.e., $E_P \simeq U$), in which case the properties of the bosonic field depend crucially on the electron correlations.

Equations (2) and (3) form the backbone of our theory. The latter can be further explicit by evaluating the Hilbert-transform of the Gaussian

$$\int dy P(y) \frac{1}{z - y} = -i \sqrt{\frac{\pi}{2\sigma^2}} \mathcal{W}\left[\frac{z}{\sqrt{2\sigma^2}}\right] \quad (6)$$

where \mathcal{W} is the complex error function.²⁸ Note also that, since the self-energy Σ does not depend on momentum, the details of the band dispersion ϵ_k enter in Eq. (2) only through the corresponding density of states. For the sake of simplicity, we shall consider a band dispersion ϵ_k with a semicircular density of states of half-width D , for which the self-consistency [Eq. (2)] reduces to $G_0^{-1} = \omega - D^2 G/4$. However, since they rely on a momentum independent quantity (the local self-energy), the results are quite independent on the choice of the band dispersion.

The spectral function, which is the quantity of interest in the present work, is defined as

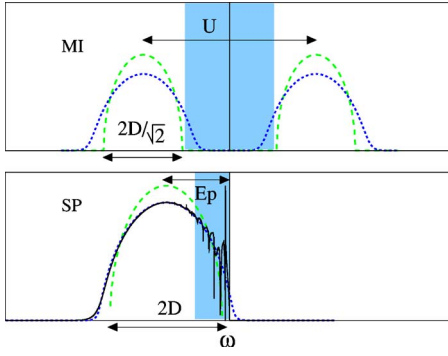


FIG. 1. (Color online) A sketch of the spectral density (the momentum-integrated spectral function). Top: In a Mott-Hubbard insulator, for $U/D=3$ without (dashed green) and with (dotted blue) electron-boson interaction ($E_p/D=0.9$, $\omega_0/D=0.1$). Bottom: In a polaronic system ($U=0$) with the same electron-boson parameters. The green dashed curve here is the noninteracting band, the black solid line is the exact DMFT result (Ref. 16) and the blue dotted curve is the approximate result based on Eq. (13). Vertical lines mark the reference energy of incoming particles. In both panels the shaded area represents the low energy part of the spectrum.

$$A(\epsilon_k, \omega) = -\frac{1}{\pi} \text{Im} \frac{1}{\omega + i\delta - \epsilon_k - \Sigma(\omega)}. \quad (7)$$

Its momentum integral—the spectral density—is $N^*(\omega) = -(1/\pi)\text{Im} G(\omega)$.

B. Mott-Hubbard insulator

For large U , and in the absence of electron-boson interactions, the set of Eqs. (1) and (2) can be rewritten as

$$\Sigma = \frac{U^2}{4 \left[\omega - \frac{D^2}{4} G \right]} \quad (8)$$

$$G \simeq \frac{1}{2} \frac{1}{\omega - \frac{D^2}{4} G \pm U/2} \quad (9)$$

The spectral density $N^*(\omega) \simeq 2/\pi D^2 \sqrt{D^2/2 - (\omega \pm U/2)^2}$ is illustrated in Fig. 1(a), and consists of two bands of reduced width $\approx 2D/\sqrt{2}$ separated by a gap $\Delta \approx U/2 - D/\sqrt{2}$ (the + and - sign are for the lower and upper Hubbard band, respectively). Such bands represent incoherent states that are strongly scattered by the disordered magnetic moments. The corresponding spectral function $A(\epsilon_k, \omega)$ exhibits broad peaks, whose width is comparable with the bandwidth itself: It is determined by the scattering rate $\Gamma(\omega) = -\text{Im} \Sigma(\omega) \sim D^2 N^*(\omega)$, which is proportional to the spectral density, and is, therefore, strongly energy dependent. As a consequence, the peaks sharpen (and become asymmetric) when approaching the band edges, as can be seen in the energy scans at constant momentum, in Fig. 2(a) (dashed green curve). Their dispersion, defined as the locus of the maxima of $A(\epsilon_k, \omega)$ at constant ω (the so-called momentum distribution curves, MDC) can be obtained by solving the equation

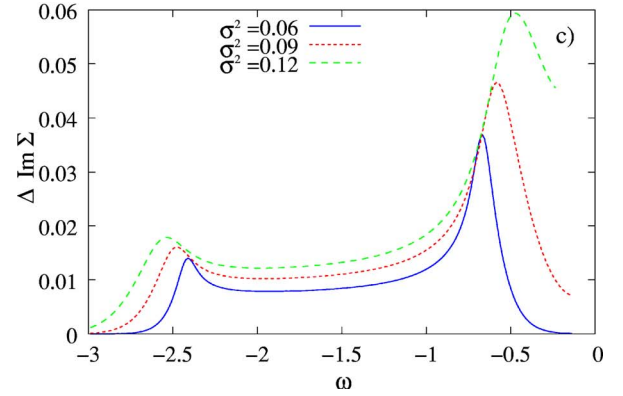
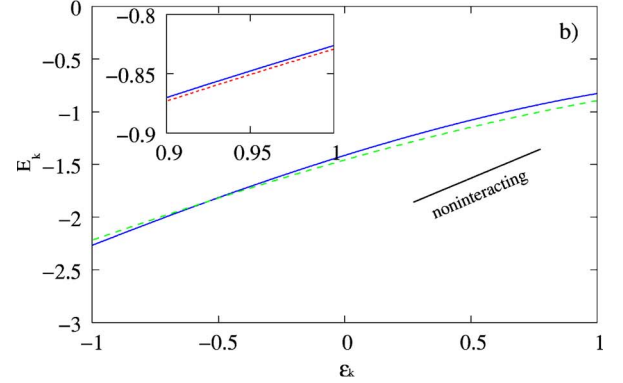
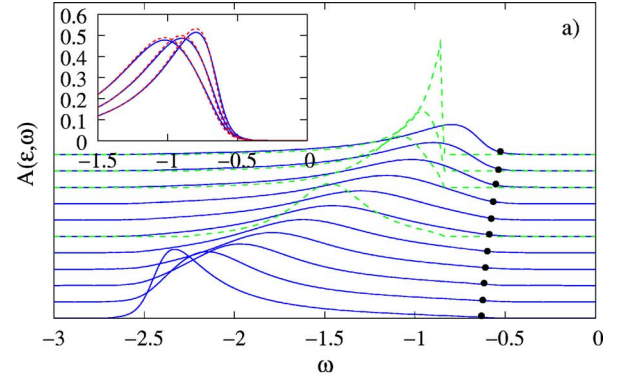


FIG. 2. (Color online) From top to bottom: (a) Energy scans of the spectral function $A(\epsilon_k, \omega)$ in a Mott-Hubbard insulator with additional electron-boson interactions, at different ϵ_k (equally spaced between the two edges $\epsilon_k = \pm D$) (solid blue lines). The parameters are $U/D=3$, $E_p/D=0.9$, $\omega_0/D=0.1$, and energies are in units of D . The curves for $\epsilon_k/D=1, 0.8, 0.6, 0.0$ in the absence of electron-boson coupling are shown for comparison (dashed green lines). The black dots mark the onset of spectral weight, which is rather dispersionless. The inset shows the effect of a shift $\Delta\omega_0/\omega_0 = -6\%$ of the boson frequency on the spectral function at the same values of ϵ_k (the dotted red line is with the modified frequency). (b) the dispersion of the broad peaks deduced from momentum scans at constant energy, for $U/D=3$ with (solid blue line) and without (dashed green line) electron-boson coupling. The slope of the noninteracting band is indicated. The inset shows the IE on the dispersion (the dotted red line is with the modified frequency). (c) Absolute value of the isotope effect on the scattering rate $\Gamma = -\text{Im} \Sigma$, defined as $\Delta\Gamma = \Gamma[\omega_0 + \Delta\omega_0] - \Gamma[\omega_0]$, for different values of $\sigma^2/D^2 = 0.06, 0.09, 0.12$.

$E_k - \text{Re} \Sigma(E_k) = \epsilon_k$, and is roughly given by $E_k = -U/2 + \epsilon_k/\sqrt{2}$ [see Fig. 2(b)].

It should be noted that the slope of the dispersion of such high energy features deviates significantly from the unrenormalized Fermi velocity v_F . For this reason, in strongly correlated electron systems, some care should be taken when extracting the function $\text{Re} \Sigma(\omega)$ from experimental data under the assumption that v_F tends asymptotically to its unrenormalized value at sufficiently high energy, as is customary in the field²⁹ (see also Ref. 30).

C. Electron-boson coupling

The coupling to a bosonic mode leads to several modifications of the picture described above. First of all, the fluctuations of the site energies lead, through the relation (3), to an overall broadening of the Hubbard bands. In particular, this generates additional exponential tails in the vicinity of the band edges, whose extension is governed by the variance $\sigma \sim \sqrt{E_P \omega_0}$. In the adiabatic regime, where the boson frequency is small compared to the bandwidth ($\omega_0 \ll D$), and for large U , such tails are typically smaller than both the width of the Hubbard bands and the size of the gap [see Fig. 1(a)].

The spectral function $A(\epsilon_k, \omega)$, for $U/D=3$ and $\sigma=0.3D$, is illustrated in Fig. 2(a) at different values of ϵ_k . This value of the variance corresponds, for example, to a moderate electron-boson coupling $E_P/D=0.9$, in the adiabatic regime $\omega_0=0.1D$ and at zero temperature. The purely electronic case ($\sigma=0$) is also shown for comparison (dashed green lines). The electron-boson coupling strongly alters the line shapes: Well inside the Hubbard bands, there is a huge broadening of the peaks, which can be estimated in the large U limit (see Appendix) to $\Delta\Gamma/\Gamma \sim 12\sigma^2/D^2$, and is of the order of 100% in the present example. However, the effect is even more dramatic in the vicinity of the band edges. There, the scattering rate, which is roughly proportional to the spectral density, has a sharp (square root) dependence on the energy in the pure electronic case, causing a marked asymmetry of the peaks. The boson fluctuations convert the sharp edge in a much smoother exponential tail, restoring a more symmetric lineshape for $A(\epsilon_k, \omega)$. Let us mention that the above-mentioned power law behavior at the edges of the Hubbard bands is not peculiar to the semicircular DOS used in this example (see Ref. 31). Indeed, analogous results are obtained starting with a flat noninteracting DOS with a step-like edge, appropriate for two-dimensional systems.

The position of the peaks is also affected by the electron-boson coupling, although to a weaker degree (this is partly in contrast with the results of Refs. 4 and 6, which only predict a broadening of the peaks, but no renormalization of the dispersion). In Fig. 2(b), we have reported the renormalized MDC dispersion E_k . The main effect of the electron-boson coupling is an increase of the slope $v_{he} = dE_k/d\epsilon_k$; its relative variation is of the order σ^2/D^2 , as can be estimated from the large U expansion presented in the Appendix, and is one order of magnitude smaller than the corresponding effect on the linewidths.

It should be noted here that, if one defines the onset of spectral weight as the locus where $A(\epsilon_k, E_k^{ons})$ equals a given

threshold (as is done, for example, in Ref. 2), the resulting E_k^{ons} appears to be almost dispersionless, as can be seen in Fig. 2(a) (black dots). This is due to the fact that the width of the peaks increases with increasing binding energy, and is ultimately related to the observation that the scattering rate is roughly proportional to the spectral density.

D. Isotope effect on the spectral properties

We shall now analyze the consequences of a change in the boson frequency on the spectral properties. Unless otherwise specified, we shall consider a relative shift $\Delta\omega_0/\omega_0 = -6\%$, that can be achieved through the substitution $^{16}\text{O} \rightarrow ^{18}\text{O}$ in the case of a lattice mode with predominantly oxygen character.³² The value inferred from the photoemission experiments in Ref. 17 on the mode at $\omega_0=70$ meV is comparable with this value, $|\Delta\omega_0|/\omega_0 \gtrsim 7\%$, pointing to a strongly phononic character of the bosonic excitation.

By direct inspection of Eq. (5), we immediately see that any isotopic effect will be strongly temperature dependent, on the scale of the boson frequency itself: At low temperatures, where $\sigma^2 = E_P \omega_0$, a modification of ω_0 directly affects the distribution (4) of the lattice displacements, and therefore, modifies the spectral properties described above. However, this effect is rapidly suppressed when the thermal fluctuations become dominant, in which case $\sigma^2 = 2E_P T$ is independent on the boson frequency. In the following, we shall present the results at $T=0$, where the IE is maximum. The IE at any temperature can be obtained straightforwardly by multiplying the results by an appropriate coefficient

$$\alpha(T) = \frac{\partial \sigma^2}{\partial \omega_0} = \left[1 - \frac{\frac{\omega_0}{T}}{\sinh \frac{\omega_0}{T}} \right] \coth \left[\frac{\omega_0}{2T} \right], \quad (10)$$

which is maximum at $T=0$ ($\alpha=1$), and rapidly drops at temperatures $T \gtrsim 0.2\omega_0$, where $\alpha \sim \omega_0/3T$.

The inset of Fig. 2(a) shows the IE on the peaks in $A(\epsilon_k, \omega)$ at various ϵ_k close to the edge of the lower Hubbard band (LHB). The reduction of the boson frequency leads to a weak shift of the peak position, corresponding to a slight reduction of the slope v_{he} , which is too weak to be observed at such moderate values of E_P [see also the inset of Fig. 2(b), where we have reported the renormalized dispersion close to the upper edge of the band]. On the other hand, we know from the previous section that the effect of the electron-boson coupling is much stronger on the linewidths than on the dispersion, and indeed some reduction of the peak widths is already visible in the plots of $A(\epsilon_k, \omega)$. For a more quantitative analysis, we have reported in Fig. 2(c) the IE on the scattering rate, defined as $\Delta\Gamma = \Gamma[\omega_0 + \Delta\omega_0] - \Gamma[\omega_0]$. It shows an interesting dependence on the energy: It is rather flat inside the Hubbard bands, but exhibits pronounced peaks of width $\sim \sigma$ around the band edges, because this is the region where the spectra are mostly affected by the bosonic fluctuations. The variation of the linewidth in the flat region well inside the Hubbard bands is approximately given by (see Appendix)

$$\frac{\Delta\Gamma_{min}}{\Delta\omega_0} \simeq 3\sqrt{2}\frac{E_P}{D} \quad (11)$$

and gives a direct measure of the strength of the electron-boson coupling. Note that although the precise numerical coefficient is specific to the semicircular DOS considered here, analogous formulas can in principle be derived for any choice of the noninteracting band (in fact, a similar result also holds in the weak coupling regime³³).

Above the band edges, the IE decays exponentially, following the fluctuation induced tails in the spectral density. This gives rise to an extremely asymmetric peak of $\Delta\Gamma$ at the band edge, which becomes more and more symmetric as σ is increased (cf. the discussion on the spectral function in the previous section). For sufficiently large $\sigma \gtrsim D$, $\Delta\Gamma(\omega)$ tends to a skewed gaussian, whose maximum is located in $\omega \simeq -U/2 + 2\sigma$, whose width is proportional to σ and height scales as

$$\frac{\Delta\Gamma_{max}}{\Delta\omega_0} \sim \sqrt{\frac{E_P}{\omega_0}}. \quad (12)$$

III. POLARONIC SEMICONDUCTOR

In this section, we use the approximate theory presented above to address the spectral properties in a system with electron-boson interactions, but in the absence of electron-electron correlations. For this problem, extensive results are available in the literature for the weak coupling regime,³³ and for the polaronic anti-adiabatic regime, where the boson frequency is assumed to be much larger than the noninteracting bandwidth.³⁵ We shall focus instead on the polaronic adiabatic regime (i.e., moderate to strong electron-boson couplings $E_P \gtrsim D$ and adiabatic bosons $\omega_0 \ll D$), which is more often encountered in solids,^{36–39} and for which a simple formulation of the spectral properties is not clearly established.

For the problem of a single electron coupled to a dispersionless boson, a complete characterization of the excitation spectrum has been given in Refs. 16 and 34 based on the dynamical mean field theory (DMFT). In the adiabatic regime, the spectra are composed of one (or several, depending on the coupling strength) narrow features at low energy, equally spaced by ω_0 , coexisting with a continuous high energy background centered around the polaron binding energy E_P . As the coupling strength increases, the low-energy features are rapidly suppressed and the spectral weight becomes dominated by the high-energy incoherent background. It should be stressed that, contrary to what happens in the anti-adiabatic limit, the high-energy features here are *dispersive* due to the strong hybridization with the free-electron states (see, e.g., Fig. 14 in Ref. 16).

The high-energy incoherent excitations are well described by an equation analogous to (3),

$$G(\Omega) = \int dy P(y) \frac{1}{G_0^{-1}(\Omega) - y}, \quad (13)$$

where the boson field obeys the same gaussian distribution of

Eq. (4). In fact, the above equation can be shown to be *rigorously* valid in the framework of the DMFT in the adiabatic limit $\omega_0=0$ [see Ref. 16 Eq. (46)]. A similar relation also holds for a system of spinless polarons at finite density,^{25,26} leading to very similar results as in the single particle case presented here.⁴¹

Note that the chemical potential is undefined in the present single particle problem. To make direct contact with the results of the previous section, we shall interpret the results for the spectral function as corresponding to the lower “Holstein band” (i.e., to excitations at negative binding energies as in a direct photoemission experiment), setting the chemical potential at the extremum of the polaron band, with the replacements $\omega = -\Omega + E_0$ and $\epsilon_k \rightarrow -\epsilon_k$ in Eq. (13). Here $E_0 \leq -D$ is the polaron binding energy taken from the DMFT solution, which tends to $-E_P$ in the strong coupling limit $E_P/D \gg 1$ (see Fig. 4 in Ref. 16).

We shall first solve the coupled equations [Eqs. (13) and (2)] in a regime where the variance σ of the boson field is smaller than the noninteracting bandwidth, which is typically the case for moderate values of the electron-boson coupling. The opposite limit $\sigma \gtrsim D$, where the spectral density takes the form of a gaussian, multiboson shakeoff peak, will be treated at the end of this section.

A. Intermediate coupling regime

The spectral density for $E_P/D=0.9$ and $\omega_0/D=0.1$ ($\sigma=0.3D$) is illustrated in Fig. 1(b) (blue dotted line). As in the correlated case, the boson fluctuations result in an overall broadening of the original band (green dashed line). The agreement with the DMFT result (black solid line) is excellent in the smooth region at high binding energies, while in the low energy region, the CPA clearly misses the detailed structure of the narrow peaks. However, even there it gives a fair description of the integrated spectral weight, which is what one would measure experimentally in the presence of a sufficient energy broadening.

1. High-energy features

The results for the spectral function are illustrated in Fig. 3(a). As in the correlated case treated in the previous section, the high energy part of the spectra is characterized by broad features, whose dispersion [Fig. 3(b)] sensibly deviates from the noninteracting case. The variation of the scattering rate under a shift of the boson frequency [Fig. 3(c)] is also very similar to the correlated case, corroborating the fact that the magnetic fluctuations only play an indirect role in the isotope effect: $\Delta\Gamma(\omega)$ is rather flat at the center of the band, and attains its maximum in a narrow region of width σ around the band edges.

For a more quantitative understanding, analytical expressions can be obtained by an expansion to lowest order in the variance, as was done previously for the Mott-Hubbard insulator. In the present case the coupled equations [Eqs. (13) and (2)] become

$$\Sigma \simeq \sigma^2 G \quad (14)$$

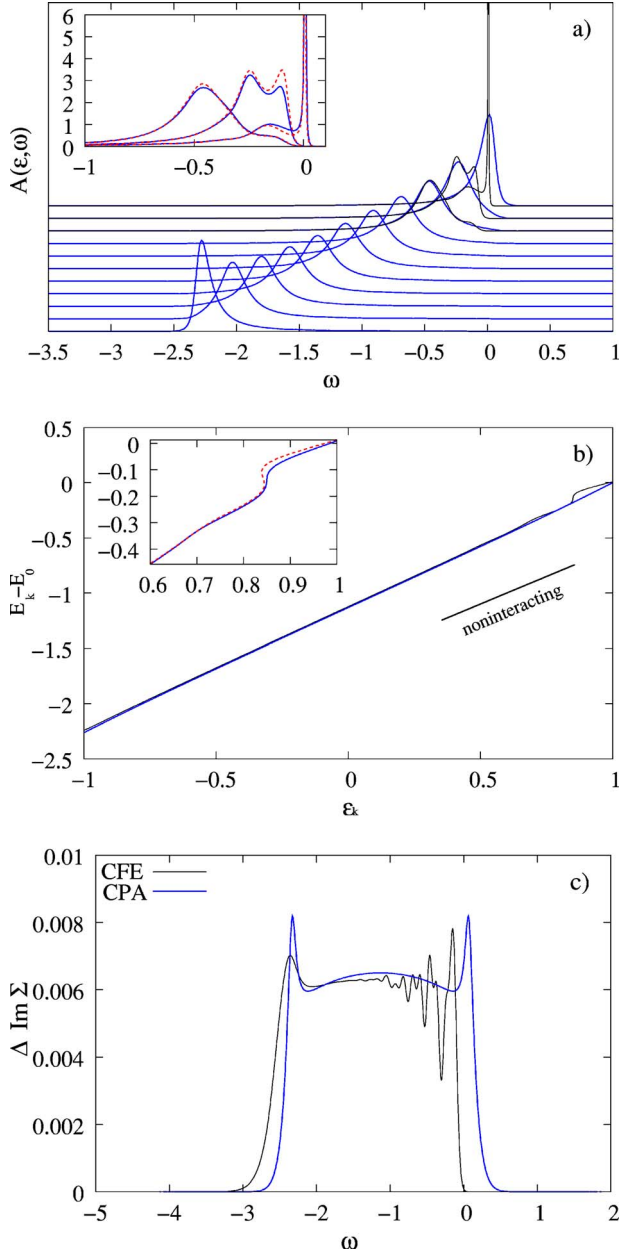


FIG. 3. (Color online) From top to bottom: (a) Energy scans of the spectral function $A(\epsilon_k, \omega)$ in a polaronic semiconductor, at different ϵ_k (equally spaced between the two edges $\epsilon_k = \pm D$) within approximation Eq. (13) (solid blue lines). The parameters are $E_P/D=0.9$, $\omega_0/D=0.1$. The curves for $\epsilon_k/D=1, 0.8, 0.6$, obtained using the exact DMFT solution, are shown for comparison (thin black lines). The inset shows the effect of a shift $\Delta\omega_0/\omega_0=-6\%$ of the boson frequency on the spectral function at the same values of ϵ_k (dotted red line is with the modified frequency). (b) The dispersion of the broad peaks deduced from momentum scans at constant energy using DMFT (thin black line) and the approximate theory (solid blue line). The slope of the noninteracting band is indicated. The inset shows the IE on the dispersion obtained in DMFT (the red dotted line is with the modified frequency). (c) Absolute value of the isotope effect on the scattering rate $\Delta\Gamma$ using DMFT (thin black line) and the approximate theory (solid blue line). Data from exact DMFT are shown after convolution with a Gaussian filter of width $0.05D$.

$$G \approx \frac{1}{\Omega - (D^2/4 + \sigma^2)G} \quad (15)$$

which is valid inside the band, far from the edges. The Green's function has the noninteracting form, but with a renormalized bandwidth given by $D \rightarrow \sqrt{D^2 + 4\sigma^2}$. The slope of the dispersion of the high-energy features is renormalized accordingly: $v_{he} = dE_k/d\epsilon_k = 1/(1 - 2\sigma^2/D^2)$, i.e., it does not coincide with the value in the absence of interactions, as can be seen in Fig. 3(b). The boson induced variation is of the same order as what was calculated in Sec. II C in the presence of electronic correlations.

From the first equation we see that the scattering rate within the band is proportional to the spectral density, $\Gamma(\Omega) \approx \pi\sigma^2 N^*(\Omega)$. Note that it is weaker than in the correlated case, due to the absence of magnetic disorder. Nevertheless, the modification of the scattering rate under a shift of the boson frequency is of the same order as in the previous case [although with a smaller prefactor, cf. Eq. (11)], namely

$$\frac{\Delta\Gamma}{\Delta\omega_0} = \frac{2E_P}{D}, \quad (16)$$

being directly proportional to the strength of the electron-boson coupling.

The existence of a maximum of $\Delta\Gamma$ near the band edge [Fig. 3(c)] also compares well with the DMFT result, although its actual position is slightly shifted to higher binding energies. This can be understood by observing that the true edge of the incoherent dispersion is at $\omega = -\omega_0$ (not at $\omega = 0$), which marks the boundary between the high-energy and low-energy regions in the excitation spectra (see below). Note that $\Delta\Gamma$ rapidly drops in the region $-\omega_0 < \omega < 0$, where Γ itself is extremely small due to our assumption of dispersionless (gapped) bosons.

2. Low-energy features

The low-energy part of the spectral function is shown in the inset of Fig. 3(a). The DMFT result shows that the broad incoherent peak progressively disappears when the band edge is approached (i.e., at low momentum transfers), while a narrow “quasi-particle” peak arises at binding energies $|\omega| < \omega_0$. The evolution of such peak-hump structure, which is characteristic of the intermediate coupling regime (in the strong coupling regime, the narrow features are too weak to be observed) causes a discontinuous jump, or kink, in the dispersion, which clearly separates the high and low-energy regions with different slopes, as illustrated in Fig. 3(b) (see also Fig. 3 in Ref. 34). The isotope effect on the kink region is shown in the inset. Note that in this plot, the isotope shift vanishes at $\omega = 0$ by definition, since the origin of energies has been shifted to coincide with the band edge (see the discussion at the beginning of this section).

B. Strong coupling limit

At extremely large values of the coupling strength $E_P/D \gtrsim D/\omega_0 \gtrsim 1$ (or at sufficiently high temperatures $T/D \gtrsim D/E_P$), the variance of the boson field can become com-

parable with the noninteracting bandwidth ($\sigma \gtrsim D$). The latter can therefore be neglected in Eq. (3), replacing $G_0^{-1} = \Omega$. Note that this does not correspond to the usual atomic, anti-adiabatic limit,³⁵ where it is assumed from the beginning that $D \rightarrow 0$ is the smallest energy scale in the problem, resulting in *dispersionless* high energy features. The present theory is valid in the opposite limit, $D \gg \omega_0$, which is more often realized in solids.^{36–38} Due to the large transfer integrals between molecular units, the discrete shakeoff spectrum characteristic of isolated molecules is converted here into a continuous Gaussian spectral density,¹⁶ and a sizeable high-energy dispersion is recovered.

We recognize from Eq. (13) that the spectral density in this case coincides with the gaussian distribution itself,

$$N^*(\omega) = P(\omega + E_p) \quad (17)$$

whose width is governed by the variance σ (we have performed the shift $\Omega = -\omega - E_p$ using the fact that $E_0 \rightarrow -E_p$ in the strong coupling limit). The full Green's function G can be read directly from Eq. (6):

$$G(\omega) = -i \sqrt{\frac{\pi}{2\sigma^2}} \mathcal{W} \left[\frac{-\omega - E_p + i\delta}{\sqrt{2\sigma^2}} \right] \quad (18)$$

At the center of the polaron peak, the self-energy $\Sigma(\omega) = -\omega - E_p - 1/G(\omega)$ tends to

$$\Sigma(\omega) = -(\omega + E_p) \left(1 - \frac{2}{\pi} \right) - i \sqrt{\frac{2\sigma^2}{\pi}} \quad (19)$$

As a consequence, the dispersion of the broad peaks in $A(\epsilon_k, \omega)$ tends to $E_k = -E_p + (\pi/2)\epsilon_k$, which defines an apparent bandwidth $= \pi D$ for the incoherent features, sensibly larger than the noninteracting value $2D$ [this should not be confused with the width of the polaron peak in the momentum-integrated spectral density of Eq. (17), which is governed by the variance σ]. Correspondingly, the slope of the high-energy dispersion saturates to a finite value in the strong electron-boson coupling limit, which is independent of the coupling strength, and is larger than the noninteracting value (cf. the opposite situation in the Mott-Hubbard insulator at strong U , Sec. II B).

In the energy interval spanned by the dispersion E_k , the scattering rate is roughly constant and directly proportional to σ . Its variation under a change of the boson frequency is given by

$$\frac{\Delta\Gamma}{\Delta\omega_0} = \sqrt{\frac{E_p}{2\pi\omega_0}}. \quad (20)$$

which is similar to the behavior encountered near the edges of the Hubbard bands [cf. Eq. (12)].

IV. CONCLUDING REMARKS

In this work, we have presented an approximate analytical theory which addresses the high energy spectral properties in systems characterized by a strong electron-boson coupling, both in the presence and in the absence of electronic correlations. Concerning the electron-boson interaction alone, the

present approach gives accurate results in the adiabatic regime (i.e., opposite to the standard strong-coupling polaron theories), where its validity can be controlled by direct comparison with the results of the dynamical mean field theory. For the correlation part, on the other hand, it reduces to the CPA treatment of Ref. 19 which qualitatively accounts for the incoherent high-energy excitations located in the upper and lower Hubbard bands.

Although the microscopic mechanisms in the cuprates certainly go beyond the simple model and approximations presented here, our results reproduce at least qualitatively several characteristics of the observed photoemission spectra, such as the existence of broad peaks with a sizeable momentum dispersion, which sharpen and become more asymmetric [in the energy distribution curve (EDC) scans] as the band edge is approached.

More specifically, we have calculated the isotope effect on the high-energy spectral features. In the present framework, where the bosonic and magnetic fluctuations are effectively decoupled, the overall behavior in the Mott insulator and in the polaronic semiconductor is qualitatively similar. The most notable result is the existence of a strongly energy dependent IE on the *linewidths*, which is maximum in a narrow energy interval of width $\sigma \sim \sqrt{E_p\omega_0}$ near the band edges, because this is the region where the excitation spectrum is mostly affected by the electron-boson interaction (new spectral weight is created there, due to the presence of boson fluctuations).

The present approach also predicts a strong temperature dependence of the IE, which should be strongly suppressed when the temperature reaches some fraction of the boson frequency (typically $T \gtrsim 0.2\omega_0$). This occurs because at high temperatures, the fluctuations of the boson field are dominated by thermal effects, which are independent on the boson frequency, and is in no way related to the existence of a temperature dependent electron-boson coupling. Note that, according to the above general arguments, an analogous energy and temperature dependence of the IE can also be expected in more accurate treatments of the electron correlations.

The results of Sec. II can be tentatively compared with the experimental results of Refs. 17 and 18. If we associate the variance σ with the observed width ~ 0.2 eV of the active IE region, and take the value $\omega_0 = 0.07$ eV for the boson energy, a "polaron" binding energy $E_p \sim 0.5$ eV is obtained. Assuming a noninteracting bandwidth of the order of 1 eV places this value in the intermediate electron-boson coupling regime. The same value of σ is also compatible with the magnitude of the observed IE on the scattering rate. From the frequency softening $\Delta\omega_0 = 5-10$ meV deduced from the shift of the kink energy, the theory predicts a decrease of the scattering rate around the band edges of the order $\Delta\Gamma \approx \sigma\Delta\omega_0/\omega_0 \sim 10-30$ meV (see the end of Sec. II D), in agreement with the experimental observations of Ref. 18.

It should be stressed that the present theory, based on a momentum independent electronic self-energy, clearly fails in addressing the strongly anisotropic *dispersion* observed in the cuprate superconductors, which demands to go beyond a local (and classical) treatment of the bosonic and magnetic fluctuations. In particular, the edges of the Hubbard bands at

low temperature are strongly affected by the “spin density wave” dispersion, especially at intermediate values of U . Another point which is beyond the range of validity of the present approach is the enhancement of the low energy IE due to proximity to a Mott metal-insulator transition. In this case, even a weak electron-boson interaction may produce a huge effect when the boson frequency is varied.¹⁵

ACKNOWLEDGMENTS

We are grateful to G. H. Gweon and A. Lanzara for sharing with us their data prior to publication. We also thank E. Cappelluti for useful discussions.

APPENDIX: IE IN THE LARGE U LIMIT

1. Inside the Hubbard bands

Well inside the LHB, we can expand (6) for small σ^2 , and neglect the effect of the UHB in Equation (3) for sufficiently large U . In the case of a semicircular DOS, we obtain

$$G \simeq \frac{1/2}{\omega - D^2G/4 + U/2} \left\{ 1 + \frac{\sigma^2}{[\omega - D^2G/4 + U/2]^2} \right\} \\ \simeq \frac{1/2}{\omega - (D^2/4 + 2\sigma^2)G + U/2} \quad (\text{A1})$$

where we have used the fact that $\omega - D^2G/4 + U/2 = 1/(2G)$ to lowest order in σ^2 . The solution for G reads

$$G(\omega) = \frac{1}{D^*2} [\omega + U/2 - \sqrt{(\omega + U/2)^2 - D^{*2}}] \quad (\text{A2})$$

with $D^{*2} = D^2/2 + 4\sigma^2$. From the self-consistency relation $G^{-1} = \omega - D^2G/4 - \Sigma$ we obtain

$$\Sigma(\omega) \simeq -\omega - U + (D^2/4 + 4\sigma^2)G(\omega) \quad (\text{A3})$$

The scattering rate $\Gamma(\omega) = -\text{Im} \Sigma(\omega)$ is, therefore, directly proportional to the spectral density at this energy. At the center of the band, it is given by

$$\Gamma = \frac{D\sqrt{2}}{4} \left[1 + \frac{12\sigma^2}{D^2} \right] \quad (\text{A4})$$

Its isotope effect at $T=0$

$$\frac{\Delta\Gamma}{\Delta\omega_0} = 3\sqrt{2} \frac{E_P}{D} \quad (\text{A5})$$

gives a direct measure of the strength of the electron-boson interaction.

2. Fluctuation induced tails

In the gap region between the Hubbard bands, additional spectral weight is created by the boson fluctuations. For small σ and sufficiently far from the band edges, both terms in (3) can be replaced by their atomic counterparts leading to the following exponential decay (for the LHB)

$$\Gamma(\omega) \simeq \sqrt{\frac{\pi}{8\sigma^2}} \frac{[\omega^2 - U^2/4]^2}{\omega^2} e^{-[\omega + U/2 - D^2\omega/4/\omega^2 - U^2/4]^2/2\sigma^2} \quad (\text{A6})$$

(note that this formula is not valid close to the band edge, i.e., where the IE is maximum).

A simpler result is obtained for sufficiently large σ , i.e., in the strong electron-boson coupling regime $U \gg \sigma^2 \gtrsim D$. In this case, the variation $\Delta\Gamma(\omega)$ of the scattering rate under a shift of the boson frequency takes the form of a skewed gaussian, which is maximum at $\omega \simeq -U/2 + 2\sigma$, where

$$\frac{\Delta\Gamma_{\max}}{\Delta\omega_0} \sim \sqrt{\frac{E_P}{\omega_0}}. \quad (\text{A7})$$

¹A. Lanzara *et al.*, Nature (London) **412**, 510 (2001).

²K. M. Shen *et al.*, Phys. Rev. Lett. **93**, 267002 (2004).

³X. J. Zhou *et al.*, Phys. Rev. Lett. **95**, 117001 (2005).

⁴O. Rösch, O. Gunnarsson, X. J. Zhou, T. Yoshida, T. Sasagawa, A. Fujimori, Z. Hussain, Z.-X. Shen, and S. Uchida, cond-mat/0504660 (unpublished).

⁵O. Rösch and O. Gunnarsson, Phys. Rev. Lett. **93**, 237001 (2004); Eur. Phys. J. B **43**, 11 (2005).

⁶A. S. Mishchenko and N. Nagaosa, Phys. Rev. Lett. **93**, 036402 (2004).

⁷H. Fehske, G. Wellein, G. Hager, A. Weisse, and A. R. Bishop, Phys. Rev. B **69**, 165115 (2004).

⁸S. Verga, A. Knigavko, and F. Marsiglio, Phys. Rev. B **67**, 054503 (2003).

⁹J. P. Hague, J. Phys.: Condens. Matter **15**, 2535 (2003).

¹⁰M. Hohenadler, M. Aichhorn, and W. von der Linden, Phys. Rev. B **68**, 184304 (2003).

¹¹T. Cuk, F. Baumberger, D. H. Lu, N. Ingle, X. J. Zhou, H. Eisaki, N. Kaneko, Z. Hussain, T. P. Devereaux, N. Nagaosa, and Z.-X.

Shen, Phys. Rev. Lett. **93**, 117003 (2004); T. P. Devereaux, T. Cuk, Z.-X. Shen, and N. Nagaosa, *ibid.* **93**, 117004 (2004).

¹²K. Ji, H. Zheng, and K. Nasu, Phys. Rev. B **70**, 085110 (2004).

¹³P. E. Kornilovitch and A. S. Alexandrov, Phys. Rev. B **70**, 224511 (2004).

¹⁴P. Paci, M. Capone, E. Cappelluti, S. Ciuchi, C. Grimaldi, and L. Pietronero, Phys. Rev. Lett. **94**, 036406 (2005).

¹⁵G. Sangiovanni, M. Capone, C. Castellani, and M. Grilli, Phys. Rev. Lett. **94**, 026401 (2005).

¹⁶S. Ciuchi, F. de Pasquale, S. Fratini, and D. Feinberg, Phys. Rev. B **56**, 4494 (1997).

¹⁷G.-H. Gweon, T. Sasagawa, S. Y. Zhou, J. Graf, H. Takagi, D.-H. Lee, and A. Lanzara, Nature (London) **430**, 187 (2004).

¹⁸G.-H. Gweon, S. Y. Zhou, M. C. Watson, T. Sasagawa, H. Takagi, and A. Lanzara (unpublished).

¹⁹J. Hubbard, Proc. R. Soc. London, Ser. A **281**, 401 (1964); R. J. Elliott, J. A. Krumhansl, and P. L. Leath, Rev. Mod. Phys. **46**, 465 (1974).

²⁰D. Vollhardt, in *Correlated Electron Systems*, edited by V. J.

- Emery (World Scientific, Singapore, 1992).
- ²¹A. Georges, G. Kotliar, W. Krauth, and M. J. Rozenberg, *Rev. Mod. Phys.* **68**, 13 (1996).
- ²²N. Bulut, D. J. Scalapino, and S. R. White, *Phys. Rev. Lett.* **73**, 748 (1994); R. Preuss, W. Hanke, and W. von der Linden, *ibid.* **75**, 1344 (1995).
- ²³M. Ulmke, R. T. Scalettar, A. Nazarenko, and E. Dagotto, *Phys. Rev. B* **54**, 16523 (1996).
- ²⁴N. Tomita and K. Nasu, *Phys. Rev. B* **60**, 8602 (1999).
- ²⁵A. J. Millis, R. Mueller, and B. I. Shraiman, *Phys. Rev. B* **54**, 5389 (1996).
- ²⁶S. Ciuchi and F. de Pasquale, *Phys. Rev. B* **59**, 5431 (1999).
- ²⁷W. Koller, D. Meyer, and A. C. Hewson, *Phys. Rev. B* **70**, 155103 (2004).
- ²⁸*Handbook of Mathematical Functions*, edited by M. Abramovitz and I. Stegun (Dover, New York, 1964).
- ²⁹T. Valla, A. V. Fedorov, P. D. Johnson, B. O. Wells, S. L. Hulbert, Q. Li, G. D. Gu, and N. Koshizuka, *Science* **285**, 2110 (1999); P. D. Johnson, T. Valla, A. V. Fedorov, Z. Yusof, B. O. Wells, Q. Li, A. R. Moodenbaugh, G. D. Gu, N. Koshizuka, C. Kendziora, S. Jian, and D. G. Hinks, *Phys. Rev. Lett.* **87**, 177007 (2001).
- ³⁰A. A. Kordyuk, S. V. Borisenko, A. Koitzsch, J. Fink, M. Knupfer, and H. Berger, *Phys. Rev. B* **71**, 214513 (2005).
- ³¹W. F. Brinkman and T. M. Rice, *Phys. Rev. B* **2**, 1324 (1970); M. E. Fisher and W. J. Camp, *ibid.* **5**, 3730 (1972).
- ³²N. N. Kovaleva, A. V. Boris, T. Holden, C. Ulrich, B. Liang, C. T. Lin, B. Keimer, C. Bernhard, J. L. Tallon, D. Munzar, and A. M. Stoneham, *Phys. Rev. B* **69**, 054511 (2004).
- ³³S. Engelsberg and J. R. Schrieffer, *Phys. Rev.* **131**, 993 (1963).
- ³⁴S. Fratini, F. de Pasquale, and S. Ciuchi, *Phys. Rev. B* **63**, 153101 (2001).
- ³⁵A. S. Alexandrov and J. Ranninger, *Phys. Rev. B* **45**, 13109 (1992); J. Ranninger, *Phys. Rev. B* **48**, 13166 (1993); G. J. Kaye, *Phys. Rev. B* **57**, 8759 (1998).
- ³⁶D. S. Dessau, T. Saitoh, C.-H. Park, Z.-X. Shen, P. Villeda, N. Hamada, Y. Moritomo, and Y. Tokura, *Phys. Rev. Lett.* **81**, 192 (1998); V. Perebeinos and P. B. Allen, *ibid.* **85**, 5178 (2000).
- ³⁷L. Perfetti, H. Berger, A. Reginelli, L. Degiorgi, H. Höchst, J. Voit, G. Margaritondo, and M. Grioni, *Phys. Rev. Lett.* **87**, 216404 (2001); L. Perfetti, S. Mitrovic, G. Margaritondo, M. Grioni, L. Forró, L. Degiorgi, and H. Höchst, *Phys. Rev. B* **66**, 075107 (2002).
- ³⁸A. Fujimori, A. E. Bocquet, K. Morikawa, K. Kobayashi, T. Saitoh, Y. Tokura, I. Hase, and M. Onoda, *J. Phys. Chem. Solids* **57**, 1379 (1996); K. Okazaki, H. Wadati, A. Fujimori, M. Onoda, Y. Muraoka, and Z. Hiroi, *Phys. Rev. B* **69**, 165104 (2004).
- ³⁹D. Schrupp, M. Sing, M. Tsunekawa, H. Fujiwara, S. Kasai, A. Sekiyama, S. Suga, T. Muro, V. A. M. Brabers, and R. Claessen, *Europhys. Lett.* **70**, 789 (2005).
- ⁴⁰A generalization of the CPA for the electron-boson interaction term has been proposed in ref. [A. C. M. Green, *Phys. Rev. B* **63**, 205110 (2001), see also Ref. 10], which in principle gives access to the narrow polaronic subbands that arise close to the Fermi level. However, such low energy excitations turn out to be totally incoherent, which constitutes an important drawback of the theory. For this reason, we restrict here to the analysis of the high energy excitations within the simplified framework of Eq. (3).
- ⁴¹In this case, the expression (3) can be rigorously derived from the Holstein model in the classical limit $M \rightarrow \infty, T \gg \omega_0$. However, contrary to the single electron case, the distribution $P(y)$ is modified by the interaction with a *finite density* of electrons. It becomes bimodal, with two peaks separated by $\Delta \sim 2E_p$, leading to an upper and a lower “Holstein band” in the spectral density (in analogy with the upper and lower Hubbard bands in correlated systems).